IEEE *Access*

Multidisciplinary : Rapid Review : Open Access Journal

An Efficient ACE Scheme for PAPR Reduction of OFDM Signals with High-order Constellation

YUZHUO LIU[1], YONG WANG[2], and BO AI[3], (Senior Member, IEEE)

Department of Communication Engineering, Xidian University, Xi'an 710071, China

Corresponding author: Yuzhuo Liu (e-mail: liu185175485@163.com).

ABSTRACT In this paper, an efficient Active Constellation Extension (ACE) based on Extension Projection Onto the Convex Sets (EPOCS-ACE) scheme is proposed for reducing Peak-to-Average Power Ratio (PAPR) of Orthogonal Frequency Division Multiplexing (OFDM) signals especially with a large number of sub-carriers and high-order constellation. Utilizing the specially designed iterative procedure, considerable PAPR reduction gains not only can be obtained with just one iteration but also can be adjusted dynamically to adapt the different designed requirements for OFDM systems. Moreover, both the novel peaks-clipping strategy and specific extension rules are designed to ensure BER performance while reducing PAPR. The theoretical analysis in terms of the selection criterion for compensation factors, optimization for correction factor, reachable bound of CCDF and computation complexity is derived. Simulation results show that, compared to existing ACE methods, EPOCS-ACE is able to obtain better overall performance in the aspect of PAPR, BER, and complexity for broadband OFDM systems.

INDEX TERMS OFDM, PAPR reduction, ACE, high-order constellation.

I. INTRODUCTION

Orthogonal Frequency Division Multiplexing (OFDM) is widely adopted in modern wireless communications because of its high spectral efficiency and transmission reliability. What's more, it has been one of the key technologies of the Fifth Generation Mobile Communication system (5G). However, being a multi-carrier modulation technique, OFDM system suffers from a critical drawback: The time-domain OFDM signal which is superimposed by several orthogonal waveforms has a variable envelope resulting in a high Peak-to-Average Power Ratio (PAPR) [1-2]. The high PAPR requires the High Power Amplifier (HPA) [3] with an extremely wide dynamic range and Digital-to-Analog converter (DAC) with high complexity. If the linear range of HPA or the accuracy of DAC is not sufficient, the high PAPR may lead to the inter-modulation among sub-carriers and undesired Out-of-Band Interference (OBI) of OFDM signals [4].

In order to reduce the envelope fluctuation of OFDM signals, a large number of PAPR reduction techniques have been proposed, which can be classified into three types: signal distortion techniques such as Clipping and Filtering (CF) [5-8], coding techniques such as Golay complementary sequences [9] or Reed-Muller code [10], and probabilistic techniques such as Selective Mapping (SLM) [11], Partial Transmit Sequence (PTS) [12-14], and

Active Constellation Extension (ACE) [15-24]. Among all these existing techniques, ACE is a promising technique that can provide high PAPR reduction gain with low system implementation complexity. Besides, it is not necessary for the transmitter to send the extra side information specially designed to help recover data at the receiver. Based on the advantages above-mentioned, ACE has been extensively used in various wireless OFDM applications, such as the second-generation European Digital Video Broadcasting Terrestrial (DVB-T2) standard [24].

ACE was first suggested in [15] by D. L. Jones. The main idea of that is to seek the optimal solution of nonlinear programming with a quadratic constraint. Considering the high complexity of the optimization procedure, the author proposed a method to obtain a suboptimal solution by iterating back and forth between two convex sets which are overlapped, namely POCS-ACE. POCS-ACE has the advantage of the perfect theoretical bound, but it requires too many iteration numbers to obtain the desired PAPR gain, resulting in slow convergence speed. Aiming at the shortcomings of POCS-ACE, Smart Gradient Project ACE (SGP-ACE) was proposed in [15] and [16] to accelerate the convergence speed by amplifying the clipping noise with a gradient step size. Nonetheless, it not only requires amounts of iterations to drop the PAPR level, but also needs an extra computation (i.e. FFTs) to obtain the appropriate gradient

step size. Under this circumstance, Least Square Approximation ACE (LSA-ACE) [23] summarizes the calculation formula of optimization factor which is equivalent to the gradient step size in SGP-ACE, thus simplifying the iterative process and greatly reducing the computation complexity. Compared with SGP-ACE and POCS-ACE, LSA-ACE performs well with just one iteration, but it sacrifices too much BER performance.

In addition to the methods mentioned above, various studies have been done to perfect the ACE technique as an ideal PAPR reduction method for OFDM systems [17-22]. For example, an ACE scheme with frame interleaving was proposed in [17] and it is very effective to reduce PAPR in OFDM systems with a small number of sub-carriers. In [18], the selection criteria of the gradient step size in SGP-ACE was further analyzed. In [19], a clipping-based ACE was proposed to tackle the low clipping ratio problem. In [20], an ACE with the bounded distortion which considers the trade-off between PAPR reduction and BER performance was proposed. In [21], a method combing Parabolic Peak Cancellation (PPC) to ACE was proposed to address the drawback of peak regrowth in traditional ACEs. In [22], a constellation extension-based method was proposed and it provides a good trade-off between complexity and performance. However, what they have done mainly focuses on ODFM systems with a small number of sub-carriers and low-order QAM.

Moreover, it should be noted that both the greater number of iterations required and the corresponding higher computation complexity are not suitable for modern OFDM systems with a large number of sub-carriers and high-order constellation. As a consequence, designing a specialized ACE scheme which can obtain a considerable PAPR gain with fast convergence speed can significantly reduce the computation complexity, and then improve its applicability for the broadband and high-rate OFDM systems.

On the other hand, ACE involves in both the peaks-clipping strategy and the constellation extension rules. For the traditional ACEs, usually, a fixed clipping threshold is set for OFDM signals with different PAPR levels, which may result in the decline of the overall performance. Meanwhile, the corresponding constellation map becomes more complex with the application of high-order QAM. The extension of internal constellation points maybe causes the sharp deterioration of BER performance. Therefore, it is necessary to design a special clipping strategy and define specific extension rules for the high-order constellation in order to ensure BER performance while reducing PAPR.

Further motivated by the investigation above, we put forward an efficient ACE scheme, namely Extension Projection Onto the Convex Sets ACE (EPOCS-ACE). Compared with the traditional ACEs, EPOCS-ACE is able to obtain the faster convergence speed with only one iteration required to approach the given PAPR level, and meanwhile the better overall performance could also be

acquired for the broadband OFDM signals employing with high-order QAM. In the proposed scheme, the original OFDM signal is amplified with an appropriate extension coefficient so as to obtain the significant PAPR gain with one single iteration. Moreover, to tackle the trade-off problem between PAPR reduction and BER performance, the self-adaption clipping strategy is used and it can dynamically adjust the clipping threshold for OFDM signals with different PAPRs. What's more, extension rules for the high-order constellation points, such as 256-QAM and 1024-QAM, are designed specially to ensure the in-band distortion does not deteriorate seriously while reducing PAPR. Furthermore, by adding a correction factor to the processing which generates the extension coefficient, the PAPR gain can be adjusted flexibly, thereby adapting various requirements of modern OFDM systems.

The following three key contributions are provided in this study:

1) The proposed scheme provides a simple formula for calculating the extension coefficient and optimizes the iteration procedure, thereby obtaining a considerable PAPR gain after just one iteration and greatly reducing the computation complexity.

2) The special extension rules for high-order QAM and the self-adaption clipping strategy are investigated to avoid a severe loss in BER performance while reducing the PAPR level.

3) The correction factor is designed innovatively so as to improve the adjustability and flexibility of the proposed scheme.

The remainder of this paper is organized as follows. Section II describes the OFDM system model and the definition of PAPR. Section III shows some details about the proposed EPOCS-ACE scheme. Section IV gives the theoretical performance analysis of EPOCS-ACE. Section V displays simulation results which compare the proposed scheme with three traditional ACEs in term of CCDF, BER, and OBI performance. Finally, the conclusions are given in section VI.

II. PAPR IN OFDM SYSTEM

In OFDM systems, an OFDM symbol consists of the sum of N signals modulated in the frequency-domain onto N different sub-carriers. Let $\mathbf{X}=[X_0, X_1, \cdots, X_{N-1}]^{\mathrm{T}}$ represent the frequency-domain data in the OFDM system with N sub-carriers. Thus, the discrete time-domain OFDM signal $\mathbf{x}=[x_0, x_1, \cdots, x_{N-1}]^{\mathrm{T}}$ can be represented as

$$ x_n = \frac{1}{\sqrt{N}} \sum_{k=0}^{N-1} X_k \cdot \exp\left(j \frac{2\pi}{N} \cdot kn \right), \quad n = 0,1,\ldots,N-1, \quad (1) $$

where n is time index and $j = \sqrt{-1}$; X_k are the complex data symbols using Phase-Shift Keying (PSK) or Quadrature Amplitude Modulation (QAM) at the kth sub-
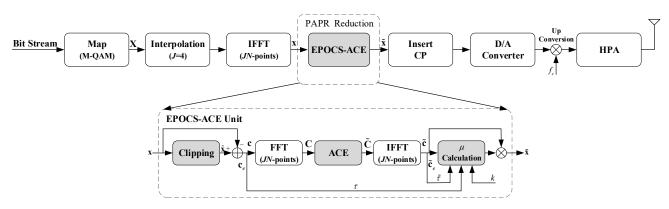
FIGURE 1. Block diagram of transmitter using EPOCS-ACE scheme; Schematic diagram of EPOCS-ACE unit.

carrier. And here, we assume the frequency-domain data X_k are statistically independent and identically distributed. The PAPR of a given symbol is mathematically defined as the ratio between the maximum instantaneous power and its average power given as follow

$$\text{PAPR}\,(\text{dB}) = 10\log\frac{\max\left\{|x_n|^2\right\}}{E\left\{|x_n|^2\right\}} = 10\log\frac{\max\limits_{0 \le n \le N}\left\{|x_n|^2\right\}}{(1/N)\sum\limits_{n=0}^{N-1}\left\{|x_n|^2\right\}}, \quad (2)$$

where $E(\cdot)$ denotes the expectation operator and $\sum(\cdot)$ represents the summation. Generally speaking, the discrete time-domain signal x_n cannot take all peaks of the continuous time-domain signal x_t, which results in the PAPR value of x_n is smaller than that of x_t. Therefore, the signal x_m which is oversampled by a factor $J(J \ge 4)$ is used to approximate the real PAPR value of x_t. The J-time over-sampled signal x_m is given by

$$x_m = \frac{1}{\sqrt{JN}}\sum_{k=0}^{JN-1} X_k' \cdot \exp\left(j\frac{2\pi}{JN} \cdot km\right), \quad m = 0, 1, \ldots, JN-1, \quad (3)$$

where X_k' is defined as

$$X_k' = \begin{cases} X_k & 0 \le k \le N/2, (JN - N/2) < k \le JN - 1 \\ 0 & other \end{cases}. \quad (4)$$

Based on the central limit theorem, when N is large enough, the real and imaginary parts of x_n are subject to Gaussian distribution, each with the zero mean and the common variance σ^2. As a result, the signal amplitude Z_n (i.e. $|x_n|$) is subject to a mutually independent Rayleigh distributions with the Probability Distribution Function (PDF) as follows

$$f_{z_n}(z) = \frac{z}{\sigma^2}\exp\left(-\frac{z^2}{2\sigma^2}\right) = 2z\exp\left(-z^2\right), \quad (5)$$

where $E\left\{Z_n^2\right\} = 2\sigma^2 = 1$.

Generally, the distribution of PAPR is measured by Complementary Cumulative Distribution Function (CCDF), which is defined as the probability that the signal's PAPR exceeds a particular threshold value $\xi_0 > 0$, i.e.

$$\text{CCDF}(\xi_0) = P_r\left(\text{PAPR} > \xi_0\right) \approx 1 - \left(1 - \exp\left(-\xi_0\right)\right)^N, \quad (6)$$

where $P_r(A)$ is the probability of the event A.

III. THE PROPOSED EPOCS-ACE SCHEME
The generic formulas and basic procedure of EPOCS-ACE scheme are presented in this section.

A. Block Diagram of EPOCS-ACE
The block diagram of an OFDM transmitter using the proposed EPOCS-ACE scheme for PAPR reduction is presented in Fig. 1. The input bit-stream data is first mapped to the complex frequency-domain data $\mathbf{X} \in \mathbb{C}^N$ by high-order QAM. Then after J-times interpolation, $\mathbf{X}$ is converted to the original oversampled time-domain signal $\mathbf{x} \in \mathbb{C}^{JN}$ using JN-points Inverse Fast Fourier Transform (IFFT). Next, $\mathbf{x}$ is given as an input to the EPOCS-ACE unit for reducing PAPR. The processed signal $\tilde{\mathbf{x}} \in \mathbb{C}^{JN}$ continues the subsequent operation until it is sent to HPA and transmitted to the wireless channel. It is worth illustrating that the EPOCS-ACE unit processes the input signal on a symbol-by-symbol basis.

As shown in Fig. 1, when the signal $\mathbf{x}$ enters the EPOCS-ACE unit, it is first processed by peaks clipping to obtain the time-domain clipping noise $\mathbf{c} \in \mathbb{C}^{JN}$. Let the set p denote the index of sample points whose amplitudes are not equal to zero in $\mathbf{c}$. Then the amplitude vector of sample points whose indexes belong to p can be denoted as $\mathbf{c}_e$. And the mean of vector $\mathbf{c}_e$ is going to be τ. Likewise, the time-domain clipping noise after the EPOCS-ACE unit is

IEEE *Access*
Multidisciplinary : Rapid Review : Open Access Journal

denoted as $\tilde{\mathbf{c}} \in \mathbb{C}^{JN}$, and the amplitude vector is denoted as $\tilde{\mathbf{c}}_e$. The mean of vector $\tilde{\mathbf{c}}_e$ is going to be $\tilde{\tau}$. Next, input the correction factor k and calculate the extension coefficient μ using the above information so as to amplify $\mathbf{x}$ with $\tilde{\mathbf{c}}$ appropriately, thereby obtaining the suppression signal $\tilde{\mathbf{x}} \in \mathbb{C}^{JN}$.

The specific procedure of EPOCS-ACE is described as follows.

Step 1. Initialize settings. Set the target of PAPR ξ_{tar} , Clipping Ratio CR_{init} , and compensation factors γ and η .

Step 2. Convert $\mathbf{X}$ to $\mathbf{x}$. And then calculate the PAPR value of $\mathbf{x}$ denoted by ξ .

Step 3. Set clipping threshold A according to CR and ξ . Then generate $\mathbf{c}$ as follows

$$\mathbf{c} = \hat{\mathbf{x}} - \mathbf{x}, \tag{7}$$

where $\hat{x}_n$ is defined as

$$\hat{x}_n = \begin{cases} x_n & |x_n| \le A \\ Ae^{j\theta_n} & |x_n| > A \end{cases}, \quad n \in [0, JN-1]. \tag{8}$$

Step 4. Let $p = \{n \mid |c_n| \ne 0\}$ and $\mathbf{c}_e = \{|c_n| \mid n \in p\}$. Then calculate τ .

Step 5. Convert $\mathbf{c}$ to frequency-domain to generate $\mathbf{C}$ using JN-points FFT. Correct $\mathbf{C}$ according to the extension rules to generate $\tilde{\mathbf{C}}$. Then convert $\tilde{\mathbf{C}}$ to time-domain to generate $\tilde{\mathbf{c}}$.

Step 6. Let $\tilde{\mathbf{c}}_e = \{|\tilde{c}_n| \mid n \in p\}$ and calculate $\tilde{\tau}$.

Step 7. Calculate μ and extend $\mathbf{x}$ as follows

$$\tilde{\mathbf{x}} = \mathbf{x} + \mu \cdot \tilde{\mathbf{c}}. \tag{9}$$

Step 8. Output $\tilde{\mathbf{x}}$ and continue the subsequent processing.

B. Self-adaption Clipping Strategy

In order to meet both PAPR and BER requirements of the OFDM system, the self-adaption clipping strategy is used in Step 3. By automatically adjusting the Clipping Ratio (*CR*) according to the PAPR value, the clipping threshold fluctuates slightly above the threshold given so as to adapt to OFDM signals with different PAPRs. The clipping threshold A is given by

$$A = \overline{\rho} \cdot 10^{\frac{CR}{20}}, \tag{10}$$

where $\overline{\rho}$ is defined as

$$\overline{\rho} = \sqrt{\frac{1}{JN} \cdot \sum_{n=0}^{JN-1} |x_n|^2}. \tag{11}$$
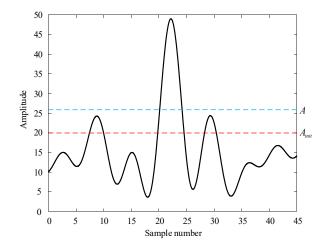

FIGURE 2. The schematic of self-adaption clipping strategy.

In the proposed scheme, the Clipping Ratio CR is corrected automatically as follows

$$CR = CR_{init} + (\gamma_{adj} - 1) \cdot \alpha \cdot (\xi - \xi_{tar}), \tag{12}$$

where γ_{adj} and α are defined as

$$\gamma_{adj} = \begin{cases} \gamma & \alpha = 1 \\ 1 & \alpha = -1 \end{cases}, \quad \alpha = \mathrm{sgn}\{(\xi - \xi_{tar}) \cdot \eta - CR_{init}\}. \tag{13}$$

In (13), γ and η are compensation factors and the selection of these depends on CR_{init} and ξ_{tar} given.

The main idea of the self-adaption clipping strategy is described as follows. Given η and let $\alpha = 0$, the upper threshold of PAPR denoted by $\xi_{thre,N}$ can be expressed as

$$\xi_{thre,N} - \xi_{tar} = \beta = \frac{CR_{init}}{\eta}, \tag{14}$$

where β is defined as a fault-tolerance range when CR takes CR_{init} . If $\xi \le \xi_{thre,N}$ (i.e. $\xi - \xi_{tar} \le \beta$), we can consider that the PAPR value is under the range which the current clipping threshold A_{init} could handle. Therefore, CR does not have to be adjusted. Otherwise, as shown in Fig. 2, it is indicated that the PAPR value is beyond the range and A_{init} is not suitable because it leads to many non-peaks are clipped. At this time, the clipping threshold should be increased to clip the target peak principally, thereby reducing the in-band distortion while dropping the PAPR level. Particularly, in the proposed scheme, CR is corrected dynamically by the difference between ξ and
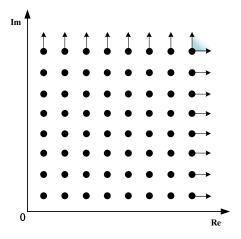
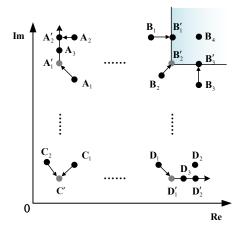**FIGURE 3.** Extension mode for the first quadrant of 256-QAM.

FIGURE 4. Specific extension rules for QAM.

ξ_{tar} of the signal so as to improve the self-adaption of the scheme.

C. Constellation Extension Rules

The extension rules for the high-order modulation in Step 5 are described in this section, and they are applicable to the modulation above 16-QAM and below 1024-QAM.

The expandable region and extension rules of ACE in Step 5 is shown in Fig. 3. If the frequency-domain constellation points after peaks clipping fall in the expandable region, these points will be retained. Otherwise, these constellation points will be extended according to the following rules. The vertex constellation points extend to the region where the shaded part is far away from the origin of the complex plane coordinate; the boundary constellation points extend away from the origin of complex plane coordinate in the direction indicated by the arrow; and the internal constellation points do not need to be extended. The detailed extension rules are shown in Fig. 4. We can

see obviously that the constellation points can be divided into two parts according to the extension mode. The internal constellation points such as C are denoted as X_k^I and the peripheral constellation points such as A, B, and D, are denoted as X_k^P. For the internal constellation points in the constellation map, the extension rules are described as follows

$$\Re\left\{\tilde{X}_k^I\right\} = \Re\left\{X_k^I\right\},$$
$$\Im\left\{\tilde{X}_k^I\right\} = \Im\left\{X_k^I\right\}. \qquad (15)$$

For the peripheral constellation points in the constellation map, the extension rules are described as follows

$$\Re\left\{\tilde{X}_k^P\right\} = \begin{cases} \Re\left\{\hat{X}_k^P\right\} & constraint\ A \\ \Re\left\{X_k^P\right\} & others \end{cases},$$
$$\Im\left\{\tilde{X}_k^P\right\} = \begin{cases} \Im\left\{\hat{X}_k^P\right\} & constraint\ B \\ \Im\left\{X_k^P\right\} & others \end{cases}. \qquad (16)$$

The *constraint A* is defined as

$$\left|\Re\left\{X_k^P\right\}\right| \geq \left|\max\left\{\Re\left\{\mathbf{X}\right\}\right\}\right|, \left|\Re\left\{\hat{X}_k^P\right\}\right| \geq \left|\Re\left\{X_k^P\right\}\right|, \quad (17)$$

and the *constraint B* is defined as

$$\left|\Im\left\{X_k^P\right\}\right| \geq \left|\max\left\{\Im\left\{\mathbf{X}\right\}\right\}\right|, \left|\Im\left\{\hat{X}_k^P\right\}\right| \geq \left|\Im\left\{X_k^P\right\}\right|. \quad (18)$$

Here, $\Re\{A\}$ and $\Im\{A\}$ are the real and imaginary part of A respectively; $\mathbf{X}$ is the original frequency-domain vector and $X_k^{\sim}$ is the kth element in $\mathbf{X}$; $\hat{X}_k^{\sim}$ and $\tilde{X}_k^{\sim}$ is the frequency-domain OFDM symbol before and after the extension operation respectively. The constellation map after extension is shown in Fig. 5.

FIGURE 5. The first quadrant of 256-QAM after extension (*N*=8192).

D. Extension Coefficient

The original time-domain signal is amplified in Step 7 by an appropriate extension coefficient, thereby accelerating the convergence speed of EPOCS-ACE. In general, the larger value of μ is, the faster convergence speed of the scheme will be. But the excessive value of μ maybe causes the peak regrowth of the non-peak points. Therefore, the proposed scheme corrects the LSA formula by adding a correction factor k to make that the corrected clipping noise $\tilde{\mathbf{c}}$ more close to the optimal clipping noise $\mathbf{c}$, consequently generating the optimal extension coefficient μ_{opt}.

The optimization objective is defined as follows

$$\mu_{opt} = \arg\min\left\{\left\|(\mu \cdot \tilde{\mathbf{c}}_e - \mathbf{c}_e) + k \cdot (\mu\tilde{\tau} - \tau) \cdot \mathbf{l}\right\|_2^2\right\}, \quad (19)$$

where $\|\mathbf{x}\|_2$ is the 2-norm of the vector $\mathbf{x}$; $\mathbf{l}$ represents a row vector whose length is the same as $\mathbf{c}_e$ and all of its elements are one. To solve the optimal solution of the above quadratic function, let

$$
\begin{aligned}
f(\mu) &= \left\|(\mu \cdot \tilde{\mathbf{c}}_e - \mathbf{c}_e) + k \cdot (\tilde{\tau} - \tau) \cdot \mathbf{l}\right\|_2^2 \\
&= \left\|\mu(\tilde{\mathbf{c}}_e + k\tilde{\tau} \cdot \mathbf{l}) - (\mathbf{c}_e + k\tau \cdot \mathbf{l})\right\|_2^2.
\end{aligned} \quad (20)
$$

Set the gradient of (20) to zero and we get the equation as follows

$$\nabla\{f(\mu)\} = 2\mu \cdot \left\|\tilde{\mathbf{c}}_e + k\tilde{\tau} \cdot \mathbf{l}\right\|_2^2 - 2(\tilde{\mathbf{c}}_e + k\tilde{\tau} \cdot \mathbf{l})(\mathbf{c}_e + k\tau \cdot \mathbf{l})^{\mathrm{T}} = 0. \quad (21)$$

Then the optimal solution of (19) is

$$\mu_{opt} = \frac{(\tilde{\mathbf{c}}_e + k\tilde{\tau} \cdot \mathbf{l})(\mathbf{c}_e + k\tau \cdot \mathbf{l})^{\mathrm{T}}}{\left\|\tilde{\mathbf{c}}_e + k\tilde{\tau} \cdot \mathbf{l}\right\|_2^2}. \quad (22)$$

As a consequence, given the value of k, the optimal extension coefficient can be calculated immediately by using (22).

IV. THEORETICAL PERFORMANCE ANALYSIS

In this section, the selection criteria of compensation factors, optimization for extension coefficient and relevant performance of EPOCS-ACE are investigated.

A. Selection Criteria of Compensation Factor

From (6), CCDF is a function of the PAPR threshold ξ_0. (6) can be rewritten as follows

$$\xi_0 = 10 \cdot \log_{10}\left\{-\ln\left(1 - \sqrt[N]{1 - \mathrm{CCDF}}\right)\right\}. \quad (23)$$

Fig. 6 plots the graph of CCDF as a function of the PAPR threshold. As shown, when CCDF starts to be less than one, the 'Theoretical' curve and the 'Simulated' curve almost
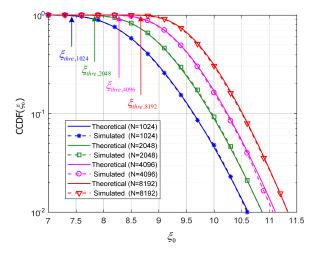

FIGURE 6. CCDF as a function of the PAPR threshold.

TABLE I
THREE SETS TYPICAL PARAMETERS FOR EPOCS-ACE SCHEME

CCDF	N	$\xi_{thre,N}$	ξ_{tar}	CR_{init}	η	γ
0.9	8192	9.125	6dB	4.68dB	1.497	1.3
0.9	8192	9.125	6dB	4.66dB	1.490	1.3
0.99	8192	8.741	6dB	4.68dB	1.707	1.3

coincide. Therefore, we define $\xi_{thre,N}$ as the PAPR value corresponding to CCDF which tends to one, i.e.

$$
\begin{aligned}
\xi_{thre,N} &= \underset{\mathrm{CCDF}\to 1}{\mathrm{l \cdot i \cdot m}}(\xi_0) \\
&= \underset{\mathrm{CCDF}\to 1}{\mathrm{l \cdot i \cdot m}}\left\{10 \cdot \log_{10}\left\{-\ln\left(1 - \sqrt[N]{1 - \mathrm{CCDF}}\right)\right\}\right\}.
\end{aligned} \quad (24)
$$

Further, the fault-tolerance range β and the compensation factor η are calculated as

$$\beta = \xi_{thre,N} - \xi_{tar} \quad (25)$$

and

$$\eta = \frac{CR_{init}}{\beta} = \frac{CR_{init}}{\xi_{thre,N} - \xi_{tar}}. \quad (26)$$

For another compensation factor γ, it determines the magnified degree of CR. Obviously, the clipping threshold is less than the maximum peak value of the signal, i.e.

$$A \le \max_{0 \le n \le JN}(|x_n|). \quad (27)$$

And the maximum CR which can be taken in ACE method is calculated as

$$CR_{\max} = 20 \cdot \log_{10}\left\{\max_{0 \le n \le JN}(|x_n|)\right\}. \quad (28)$$
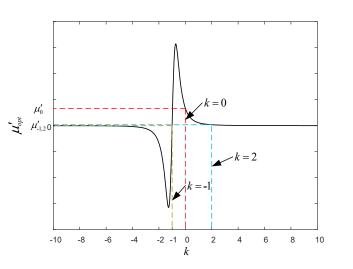
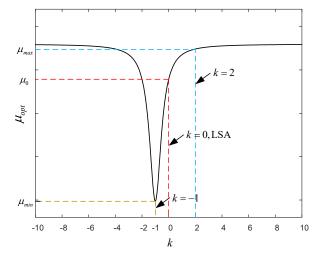FIGURE 7. μ'_{opt} as a function of *k*.

FIGURE 8. μ_{opt} as a function of *k*.

As a result, the range of γ can be given by

$$1 \leq \gamma \leq \frac{CR_{\max} - CR_{init}}{\xi - \xi_{tar}} + 1. \tag{29}$$

Usually, in order to ensure the suppression effect of PAPR, A_{init} is set to be a value which is less than $2\overline{\rho}$. Then the maximum range of γ used in the proposed scheme is given as follows

$$1 \leq \gamma \leq \frac{CR_{\max} - 20 \cdot \log_{10} 2}{\xi - \xi_{tar}} + 1. \tag{30}$$

Three sets of typical parameters are presented in TABLE I for the verification and following simulations.

B. Optimization for Extension Coefficient

From (22), we can see that μ_{opt} is a function of the correction factor k. In order to seek a suitable range of k, (22) can be transformed into (31) as follow.

$$\mu_{opt} = \frac{k^2 \left(\tilde{\tau}\tau \cdot \mathbf{1} \cdot \mathbf{1}^{\mathrm{T}} \right) + k \left(\tau \cdot \tilde{\mathbf{c}}_e + \tilde{\tau} \cdot \mathbf{c}_e \right) \cdot \mathbf{1}^{\mathrm{T}} + \tilde{\mathbf{c}}_e \cdot \mathbf{c}_e^{\mathrm{T}}}{k^2 \left(\tilde{\tau}^2 \cdot \mathbf{1} \cdot \mathbf{1}^{\mathrm{T}} \right) + k \left(2\tilde{\tau} \cdot \tilde{\mathbf{c}}_e \cdot \mathbf{1}^{\mathrm{T}} \right) + \tilde{\mathbf{c}}_e \cdot \tilde{\mathbf{c}}_e^{\mathrm{T}}}. \tag{31}$$

The derivation of the above function's properties is detailed in the Appendix and μ'_{opt} is given by (A-6). Fig. 7 plots the graph of μ'_{opt} as the function of k. As shown, when $k = -1$, $\mu'_{opt} = 0$ and when $k \geq 2$, the value of μ'_{opt} is going to zero. Meanwhile, when $k \in (-1, 2)$, $\mu'_{opt} > 0$. Hence, when $k \in [-1, 2]$, the value of μ_{opt} should increase along with k.

The graph of μ_{opt} as the function of k is shown in Fig. 8. As observed, when $k \in [-1, 0]$, the value of μ_{opt} increases quickly along with k. When $k \in [0, 2]$, the increase rate of μ_{opt} start slowing down. And when $k \in [2, +\infty]$, the value of μ_{opt} no longer increases along with k. Hence, the suitable range of k in EPOCS-ACE should be $k \in [-1, 2]$. Meanwhile, the range of μ_{opt} can be obtained as

$$\frac{\left(\tilde{\mathbf{c}}_e - \tilde{\tau} \cdot \mathbf{1} \right) \left(\mathbf{c}_e - \tau \cdot \mathbf{1} \right)^{\mathrm{T}}}{\left\| \tilde{\mathbf{c}}_e - \tilde{\tau} \cdot \mathbf{1} \right\|_2^2} \leq \mu_{opt} \leq \frac{\left(\tilde{\mathbf{c}}_e + 2\tilde{\tau} \cdot \mathbf{1} \right) \left(\mathbf{c}_e + 2\tau \cdot \mathbf{1} \right)^{\mathrm{T}}}{\left\| \tilde{\mathbf{c}}_e + 2\tilde{\tau} \cdot \mathbf{1} \right\|_2^2}. \tag{32}$$

When $k = 0$, that value of μ_0 is given by

$$\mu_0 = \frac{\tilde{\mathbf{c}}_e \cdot \mathbf{c}_e^{\mathrm{T}}}{\left\| \tilde{\mathbf{c}}_e \right\|_2^2}. \tag{33}$$

Consequently, both LSA-ACE and POCS-ACE can be considered as two special cases of the proposed scheme, i.e. when $k = 0$ and $\mu_{opt} = 1$ respectively.

C. Reachable CCDF

The PAPR of the proposed scheme is defined as follows.

$$\mathrm{PAPR\,(dB)} = 10 \log \frac{\max\limits_{0 \leq n \leq JN} \left\{ \left| x_n + \mu \cdot \tilde{c}_n \right|^2 \right\}}{(1/JN) \sum\limits_{n=0}^{JN-1} \left\{ \left| x_n + \mu \cdot \tilde{c}_n \right|^2 \right\}} \tag{34}$$

For an OFDM symbol, amplifying the clipping noise is equivalent to reducing the clipping threshold. Thus, when $k \in [-1, 2]$, the value of PAPR decreases along with the increase of k. If the maximal value of PAPR (i.e. $k = -1$)
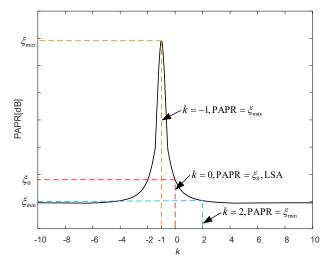
FIGURE 9. PAPR as a function of k for an OFDM symbol ($\gamma = 1$).

is denoted as $\xi_{\max}$ and the minimal value (i.e. $k = 2$) is denoted as $\xi_{\min}$, then the theoretical reachable bound of CCDF can be further expressed as

$$1 - \left(1 - \exp\left(-\xi_{\max}\right)\right)^{JN} \leq \text{CCDF} \leq 1 - \left(1 - \exp\left(-\xi_{\min}\right)\right)^{JN}. \quad (35)$$

Fig. 9 plots the graph of PAPR as the function of k for an OFDM symbol. Based on Fig. 8 and Fig. 9, within the appropriate CR range, the greatest PAPR reduction gain of EPOCS-ACE is obtained when $k = 2$, and it is better than that of LSA-ACE under the same condition. Moreover, the PAPR gain can be dynamically adjusted with the value of k. Particularly, it is noteworthy that though the PAPR value of signal is fluctuating, the PAPR gain obtained by EPOCS-ACE can be forecasted roughly based on Fig. 9. Thus, it is novel if the overall performance of OFDM systems can be predicted before the ACE processing.

D. Computation Complexity

The computation complexity of the proposed scheme mainly focuses on the IFFT/FFT operation and calculation for the extension coefficient. For an OFDM system with N sub-carriers, the number of elements which are in the vector $\mathbf{c}_e$ and vector $\tilde{\mathbf{c}}_e$ are much smaller than N. As a result, the computation complexity which is generated by calculating the extension coefficient is far less than that of IFFT/FFT operations. The complexity of the addition and the multiplication operation of each JN-points IFFT/FFT operation can be calculated as

$$n_{add} = JN \cdot \log_2 JN \quad (36)$$

and

TABLE II
COMPLEXITY COMPARISON FOR ACEs ABOVE-MENTIONED

Method Name	n_{Tadd}	n_{Tmul}
EPOCS-ACE	$2JN \cdot \log_2 JN$	$JN \cdot \log_2 JN$
LSA-ACE	$2JN \cdot \log_2 JN \cdot iter$	$JN \cdot \log_2 JN \cdot iter$
SGP-ACE	$3JN \cdot \log_2 JN \cdot iter$	$1.5JN \cdot \log_2 JN \cdot iter$
POCS-ACE	$2JN \cdot \log_2 JN \cdot iter$	$JN \cdot \log_2 JN \cdot iter$

$$n_{mul} = \left(JN/2\right) \cdot \log_2 JN. \quad (37)$$

As can be seen from the procedure of EPOCS-ACE, the only one IFFT operation and one FFT operation are included. Therefore, the computation complexity of EPOCS-ACE can be determined by

$$n_{Tadd} = 2JN \cdot \log_2 JN \quad (38)$$

and

$$n_{Tmul} = JN \cdot \log_2 JN, \quad (39)$$

where n_{Tadd} represents the total number of the addition operations and n_{Tmul} is the total number of the multiplication operations. With regard to the oversampling OFDM signal, the computation complexity of each method mentioned above is shown in TABLE II.

From TABLE II, we can observe that increasing iteration numbers means increasing the computation complexity, especially when the number of sub-carriers is very large. However, as this paper shows later, EPOCS-ACE can obtain a considerable PAPR gain with just one iteration, dramatically decreasing the number of required iterations. For one iteration, the computation complexity of EPOCS-ACE is nearly the same as that of POCS-ACE and LSA-ACE, but far less than that of SGP-ACE. In fact, on account of the slow convergence speed of POCS-ACE, a lot of iterations are required to drop PAPR below the desired level. As a result, given the same target of PAPR, the computation complexity of POCS-ACE far outstrips that of EPOCS-ACE.

V. SIMULATION RESULTS

In this section, the overall performance of EPOCS-ACE scheme is evaluated and compared with traditional ACEs. Simulations are performed for an un-coded OFDM system with a large number of sub-carriers and the high-order modulation at the transmitter. And we assume that OFDM symbol timing is ideal, the carrier frequency offset is absent and the perfect channel estimation is performed at the receiver. For comparisons, three classic ACEs including POCS-ACE, SGP-ACE, and LSA-ACE are considered with

TABLE III
SIMULATION PARAMETERS FOR TRADITIONAL ACEs

Parameter	N	M-QAM	J	ξ_{tar}	CR/CR_{init}
Value	8192	256/1024-QAM	4	6dB	4.68dB/4.66dB

TABLE IV
SIMULATION PARAMETERS FOR EPOCS-ACE SCHEME

Parameter	N	M-QAM	J	ξ_{tar}	CR/CR_{init}	k	η	γ
Value	8192	256/1024-QAM	4	6dB	4.68dB/4.66dB	2	1.497/1.490	1.3

their PAPR reduction, BER and OBI performance. Particularly, since extension rules for the high-order constellation are not defined in previous three ACEs, the extension rules proposed in the paper are used for each method. The detailed simulation parameters for traditional ACEs (i.e. POCS, SGP, and LSA) and EPOCS-ACE are shown in TABLE III and TABLE IV respectively.

A. PAPR Reduction

Fig. 10 and Fig. 11 plot CCDFs of the PAPR for the original OFDM symbol and processed symbol, which are modulated by 256-QAM and 1024-QAM respectively, with different ACE methods. And "i" is the iteration number for each method. From these figures, we can observe that the convergence speed of EPOCS-ACE is obviously faster than that of other methods after a single iteration. And the proposed scheme can significantly achieve a sharp drop in CCDF with only one iteration. For example, given that CCDF=10^{-4} for 256-QAM, the PAPR reduction gain of about 1.80dB can be obtained after sixty iterations using POCS-ACE. For SGP-ACE and LSA-ACE, the PAPR reduction gain of about 3.10dB can be obtained after one iteration respectively; and that of about 3.20dB and 3.05dB can be obtained after two iterations respectively. However, for EPOCS-ACE, the PAPR reduction gain of about 3.90dB can be obtained after only one iteration. Consequently, EPOCS-ACE performs better in PAPR reduction than traditional ACEs above-mentioned.

Compared Fig. 11 with Fig. 10, for 1024-QAM, the PAPR suppression effect of SGP-ACE and LSA-ACE deteriorates seriously. However, that of EPOCS-ACE is still outstanding due to the special optimal strategy.

Fig. 12 plots CCDFs of PAPR for EPOCS-ACE with different input k. And the pink curve marked with 'TUB' in the figure is the upper bound of PAPR suppression effect for EPOCS-ACE. As shown, when $k \leq 0$, the PAPR suppression effect increases quickly along with k. When $k > 0$ and particularly $k \to 2$, the increasing speed levels off gradually. When $k = 2$, the proposed scheme achieves the greatest PAPR suppression effect on the signal. This phenomenon is consistent with the influence of the value of k on PAPR reduction, which is analyzed in the previous paragraph.
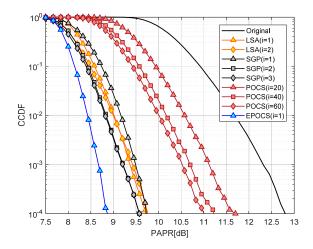

FIGURE 10. CCDF statistics of OFDM signal with different ACE PAPR reduction schemes (Un-coded 256-QAM, γ = 1.3, η =1.497).
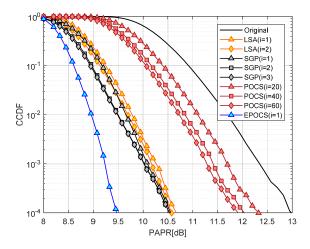

FIGURE 11. CCDF statistics of OFDM signal with different ACE PAPR reduction schemes (Un-coded 1024-QAM, γ = 1.3, η = 1.490).

B. BER Performance

Fig. 13 and Fig. 14 depict the BER versus E_b/N_0 corves of OFDM symbol for different ACEs through an AWGN channel for 256-QAM and 1024-QAM respectively. As a reference, the black curve marked with 'Original' in the
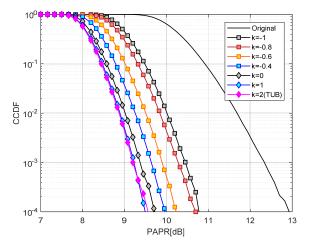
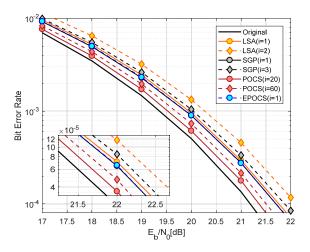**FIGURE 12.** CCDF statistics for EPOCS-ACE scheme with different k (Un-coded 256-QAM, $\gamma = 1$).

FIGURE 14. BER performance comparison for different ACE PAPR reduction schemes through AWGN channel for OFDM system (Un-coded 1024-QAM, $\gamma = 1.3$, $\eta = 1.490$).

FIGURE 13. BER performance comparison for different ACE PAPR reduction schemes through AWGN channel for OFDM system (Un-coded 256-QAM, $\gamma = 1.3$, $\eta = 1.497$).

FIGURE 15. Simulated PSDs of different ACE PAPR reduction schemes for OFDM system (Un-coded 256-QAM, $\gamma = 1.3$, $\eta = 1.497$).

figure is the ideal theoretical BER curve of the original OFDM signal passing through the AWGN channel. As shown, while we increase the iterative numbers of each method, the corresponding BER performance gradually becomes poor because of the amplification of the clipping noise.

However, a better BER performance of EPOCS-ACE can be offered when compared with other referred methods with a single iteration for a given BER level. For example, to guarantee BER=10^{-4} for 256-QAM, the required E_b/N_0 for EPOCS-ACE increases about 0.5dB after one iteration, which is superior to that of LSA-ACE after one iteration and SGP-ACE after three iterations respectively. Considering the PAPR reduction gain brought by the proposed scheme, the loss of BER performance is within the acceptable range.
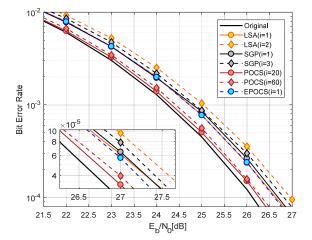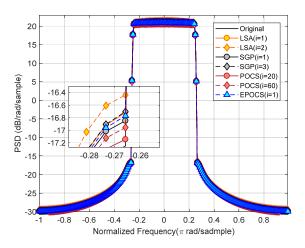
C. OBI Performance

The simulated Power Spectral Densities (PSDs) of an OFDM system using different ACE methods are depicted in Fig. 15. As shown, because of the peaks-clipping operation in the time-domain, the PSD curves of the output signals for each method expend outwards, resulting in slightly out-of-band interference. As can be seen form Fig. 15, the OBI of POCS-ACE is minimal after twenty iterations and that of LSA-ACE is maximal after two iterations. After one iteration, the OBI of EPOCS-ACE is the same as that of LSA-ACE. And EPOCS-ACE leads to about 0.48dB out-of-band spectral regrowth compared with that of the original OFDM symbol at the normalized frequency of 0.265. Therefore, that confirms the OBI performance meets the desired requirements of OFDM systems.

In summary, compared with traditional ACEs, the proposed scheme can obtain more significant PAPR gains with lower computation complexity, at the price of the acceptable BER and OBI performance.

VI. CONCLUSION

In this paper, an EPOCS-ACE scheme has been proposed to reduce PAPR of OFDM signals. EPOCS-ACE makes a novel extension rules for high-order constellation points to adapt to existing OFDM systems with a large number of sub-carries and high transmission rate. Meanwhile, it can also obtain a fast convergence speed with just one iteration. What's more, an additional advantage of EPOCS-ACE is the PAPR gain can be forecasted roughly and adjusted dynamically so as to improve the flexibility for parameters selection of OFDM systems. The comprehensive theoretical analysis is derived and the analytical results regarding the selection criterion for the compensation factors and correction factor, theoretical bound, and computation complexity are presented. Simulation results demonstrate that, compared to existing ACEs, EPOCS-ACE exhibits a better overall performance, including the excellent PAPR gains, acceptable loss of BER performance, and low computation complexity for broadband OFDM systems.

APPENDIX

The optimal extension coefficient μ_{opt} is a function of the correction factor k. In order to analyze the properties of this function and obtain the appropriate range of k, (22) can be rewritten as

$$\mu_{opt} = \frac{k^2\left(\tilde{\tau}\tau\cdot\mathbf{1}\cdot\mathbf{1}^{\mathrm{T}}\right)+k\left(\tau\cdot\tilde{\mathbf{c}}_e+\tilde{\tau}\cdot\mathbf{c}_e\right)\cdot\mathbf{1}^{\mathrm{T}}+\tilde{\mathbf{c}}_e\cdot\mathbf{c}_e^{\mathrm{T}}}{k^2\left(\tilde{\tau}^2\cdot\mathbf{1}\cdot\mathbf{1}^{\mathrm{T}}\right)+k\left(2\tilde{\tau}\cdot\tilde{\mathbf{c}}_e\cdot\mathbf{1}^{\mathrm{T}}\right)+\tilde{\mathbf{c}}_e\cdot\tilde{\mathbf{c}}_e^{\mathrm{T}}}. \quad (A\text{-}1)$$

Suppose the length of the clipping amplitude vectors $\mathbf{c}_e$ and $\tilde{\mathbf{c}}_e$ is l. $\mathbf{c}_e$ and $\tilde{\mathbf{c}}_e$ can be defined as follow.

$$\begin{cases}\mathbf{c}_e=\left[c_0,c_1,\cdots,c_{l-1}\right]^{\mathrm{T}}\\\tilde{\mathbf{c}}_e=\left[\tilde{c}_0,\tilde{c}_1,\cdots,\tilde{c}_{l-1}\right]^{\mathrm{T}}\end{cases} \quad (A\text{-}2)$$

Then we can get

$$\begin{cases}\mathbf{1}\cdot\mathbf{1}^{\mathrm{T}}=l\\\tau=\dfrac{c_0+c_1+\cdots+c_{l-1}}{l}\\\tilde{\tau}=\dfrac{\tilde{c}_0+\tilde{c}_1+\cdots+\tilde{c}_{l-1}}{l}\\\mathbf{c}_e\cdot\mathbf{1}^{\mathrm{T}}=c_0+c_1+\cdots+c_{l-1}=l\tau\\\tilde{\mathbf{c}}_e\cdot\mathbf{1}^{\mathrm{T}}=\tilde{c}_0+\tilde{c}_1+\cdots+\tilde{c}_{l-1}=l\tilde{\tau}\end{cases} \quad (A\text{-}3)$$

Substitute (A-3) into (A-1), and the numerator and the denominator simultaneously are proposed the coefficient of k^2. Then the (A-1) can be simplified as

$$\mu_{opt}=\frac{\tau}{\tilde{\tau}}\left(\frac{k^2+2k+\dfrac{\tilde{\mathbf{c}}_e\cdot\mathbf{c}_e^{\mathrm{T}}}{\tilde{\tau}\tau\cdot l}}{k^2+2k+\dfrac{\tilde{\mathbf{c}}_e\cdot\tilde{\mathbf{c}}_e^{\mathrm{T}}}{\tilde{\tau}^2\cdot l}}\right)=\frac{\tau}{\tilde{\tau}}\left(1+\frac{\dfrac{\tilde{\mathbf{c}}_e\cdot\mathbf{c}_e^{\mathrm{T}}}{\tilde{\tau}\tau\cdot l}-\dfrac{\tilde{\mathbf{c}}_e\cdot\tilde{\mathbf{c}}_e^{\mathrm{T}}}{\tilde{\tau}^2\cdot l}}{k^2+2k+\dfrac{\tilde{\mathbf{c}}_e\cdot\tilde{\mathbf{c}}_e^{\mathrm{T}}}{\tilde{\tau}^2\cdot l}}\right).\,(A\text{-}4)$$

Furthermore, (A-4) can be simplified as

$$\mu_{opt}=\frac{\tau}{\tilde{\tau}}\left\{1+\left(\frac{\tilde{\mathbf{c}}_e\cdot\mathbf{c}_e^{\mathrm{T}}\cdot\tilde{\tau}-\tilde{\mathbf{c}}_e\cdot\tilde{\mathbf{c}}_e^{\mathrm{T}}\cdot\tau}{\tilde{\tau}^2\tau\cdot l}\right)\cdot\left(\frac{1}{k^2+2k+\dfrac{\tilde{\mathbf{c}}_e\cdot\tilde{\mathbf{c}}_e^{\mathrm{T}}}{\tilde{\tau}^2\cdot l}}\right)\right\}.$$
$$(A\text{-}5)$$

From (A-5), the derivative of μ_{opt} with respect to k is given by

$$\mu_{opt}'=\frac{\tau}{\tilde{\tau}}\left\{\left(\frac{\tilde{\mathbf{c}}_e\cdot\tilde{\mathbf{c}}_e^{\mathrm{T}}\cdot\tau-\tilde{\mathbf{c}}_e\cdot\mathbf{c}_e^{\mathrm{T}}\cdot\tilde{\tau}}{\tilde{\tau}^2\tau\cdot l}\right)\cdot\left(\frac{2(k+1)}{\left(k^2+2k+\dfrac{\tilde{\mathbf{c}}_e\cdot\tilde{\mathbf{c}}_e^{\mathrm{T}}}{\tilde{\tau}^2\cdot l}\right)^2}\right)\right\}.$$
$$(A\text{-}6)$$

In (A-6),

$$\begin{aligned}\tilde{\mathbf{c}}_e\cdot\tilde{\mathbf{c}}_e^{\mathrm{T}}\cdot\tau-\tilde{\mathbf{c}}_e\cdot\mathbf{c}_e^{\mathrm{T}}\cdot\tilde{\tau}&=\sum_{i=0}^{l-1}\tilde{c}_i^2\cdot\sum_{j=0}^{l-1}c_j-\sum_{i=0}^{l-1}\tilde{c}_ic_i\cdot\sum_{j=0}^{l-1}\tilde{c}_j\\&=\sum_{i=0,i\neq j}^{l-1}\sum_{j=0,i\neq j}^{l-1}\left(\tilde{c}_i^2c_j-\tilde{c}_ic_i\tilde{c}_j\right).\end{aligned} \quad (A\text{-}7)$$

Let $c_{\min}=\min\left(c_0,c_1\cdots,c_{l-1}\right)>0$, then

$$\begin{aligned}\sum_{i=0,i\neq j}^{l-1}\sum_{j=0,i\neq j}^{l-1}\left(\tilde{c}_i^2c_j-\tilde{c}_ic_i\tilde{c}_j\right)&\geq\sum_{i=0,i\neq j}^{l-1}\sum_{j=0,i\neq j}^{l-1}\left(\tilde{c}_i^2-\tilde{c}_i\tilde{c}_j\right)\cdot c_{\min}\\&\geq\sum_{i=0,i\neq j}^{l-1}\sum_{j=0,i\neq j}^{l-1}\left(\tilde{c}_i-\tilde{c}_j\right)^2\cdot c_{\min}\\&\geq 0.\end{aligned} \quad (A\text{-}8)$$

Therefore, we can get

$$\frac{\tilde{\mathbf{c}}_e\cdot\tilde{\mathbf{c}}_e^{\mathrm{T}}\cdot\tau-\tilde{\mathbf{c}}_e\cdot\mathbf{c}_e^{\mathrm{T}}\cdot\tilde{\tau}}{\tilde{\tau}^2\tau\cdot l}\geq 0. \quad (A\text{-}9)$$

Let $\mu_{opt}'=0$, then $k=-1$. When $k>-1$, $\mu_{opt}'>0$. Then the value of μ_{opt} increases along with the k. Usually, the element value in vector $\tilde{\mathbf{c}}_e$ is very small. The value of the denominator in (A-6) is mainly determined by that of k. When $k\geq 2$, μ_{opt}' is going to zero. As a result, when we increase the value of k, μ_{opt} is no longer increased. Therefore, the suitable range of k in proposed scheme should be $k\in\left[-1,2\right]$.

REFERENCES

[1] L. Hanzo, M. Munster, B. J. Choi, and T. Keller, "OFDM and MC-CDMA for broadband multi-user communications," *WLANs and Broadcasting, Chichester*, England: John Wiley & Sons, 2003.

[2] F. B. Offiong, S. Sinanovic, and W. Popoola, "On PAPR reduction in Pilot-Assisted optical OFDM communication systems," *IEEE Access*, vol. 5, pp. 8916–8929, May 2017.

[3] K. Anoh, K. M. Rabie, B. Adebisi, and C. Tanriover, "Root-based nonlinear companding technique for reducing PAPR of precoded OFDM signals," *IEEE Access*, vol. 6, pp. 4618–4629, Dec. 2017.

[4] T. Hwang, C. Yang, G. Wu, S. Li, and G. Y. Lee, "OFDM and its wireless application: A survey," *IEEE Trans. Veh. Technol.*, vol. 58, no. 4, pp. 1673–1694, May 2009.

[5] L. Wang and C. Tellambura, "A simplified clipping and filtering technique for PAR reduction in OFDM Systems," *IEEE Signal Process. Lett.*, vol. 12, no. 6, pp. 453–456, Jun. 2005.

[6] A. Ali, A. Al-Rabah, M. Masood, and T. Y. Al-Naffouri, "Receiver-Based recovery of clipped OFDM signals for PAPR reduction: A bayesian approach," *IEEE Access*, vol. 2, pp. 1213–1224, Oct. 2014.

[7] K. Anoh, C. Tanriover, B. Adebisi, and M. Hammoudeh, "A new approach to iterative Clipping and Filtering PAPR reduction scheme for OFDM systems," *IEEE Access*, vol. 6, pp. 17533–17544, Sep. 2017.

[8] X. Liu, X. Zhang, Jun X., F. Gu, and J. Wei, "An enhanced iterative Clipping and Filtering method using time-domain Kernel Matrix for PAPR reduction in OFDM systems," *IEEE Access*, vol. 7, pp. 59466–59476, May 2019.

[9] M. Golay, "Complementary Series, Information Theory," *IEEE Trans. Inf. Theory*, vol. 7, no. 2, pp. 83–87, 1961.

[10] K. G. Paterson, "Generalized reed-muller codes and power control in OFDM Modulation," *IEEE Trans. Inf. Theory*, vol. 46, no. 1, pp. 104–120, Jan. 2000.

[11] J. Yang, L. Chen, Q. Liu, and D. Chen, "A modified Selected Mapping Technique to reduce the Peak-to-Average Power Ratio of OFDM signals," *IEEE Trans. Consum. Electron.*, vol. 53, no. 3, pp. 846–851, Aug. 2007.

[12] H. Wang, X. Wang, L. Xu, and W. Du, "Hybrid PAPR reduction scheme for FBMC/OQAM systems based on multi data block PTS and TR methods," *IEEE Access*, vol. 4, pp. 4761–4768, Sep. 2016.

[13] P. Varahram and B. M. Ali, "Partial Transmit Sequence scheme with new phase sequence for PAPR reduction in OFDM systems," *IEEE Trans. Consum. Electron.*, vol. 57, no. 2, pp. 366–371, May 2011.

[14] Y. A. Jawhar, L. Audah, M. A. Taher, K. N. Ramli, and M. Sami, "A review of Partial Transmit Sequence for PAPR reduction in the OFDM systems," *IEEE Access*, vol.7, pp. 18021–18041, Feb. 2019.

[15] B. S. Krongold and D. L. Jones, "PAR reduction in OFDM via Active Constellation Extension," *IEEE Trans. Broadcast.*, vol. 49, no. 3, pp. 258–268, Sep. 2003.

[16] B. S. Krongold, "New techniques for multicarrier communication system," *University of Illinois*, 2003.

[17] Z. Yang, H. Fang, and C. Pan, "ACE with frame interleaving scheme to reduce peak-to-average power ratio in OFDM systems," *IEEE Trans. Broadcast.*, vol. 51, no 4, pp. 571–575, Dec. 2005.

[18] L. Wang and C. Tellambura, "An adaptive-scaling algorithm for OFDM PAR reduction using Active Constellation Extension" in *Proceedings of the 64th IEEE Vehicular Technology Conference, (VTC)*, Montréal, Québec, Canada, Sep. 25–28, 2006.

[19] K. Bae, J. G. Andrews, and E. J. Powers, "Adaptive active constellation extension algorithm for peak-to-average ratio reduction in OFDM," *IEEE Commun. Lett.*, vol. 14, no. 1, pp. 0–41, Jan. 2010.

[20] S. K. Deng and M. C. Lin, "OFDM PAPR reduction using clipping with distortion control" in *IEEE international conference on communications, (ICC)*, Seoul, Korea, May. 16-20, 2005.

[21] J. Liu, M. Yu, X. Zeng, M. Wang, and J. Lu, "A method of combining PPC and ACE to reduce PAPR in CO-OFDM system," in *Asia Communications and Photonics Conference, (ACP)*, Beijing, China, 2013.

[22] M. C. P. Paredes, J. J. Escuderogarzas, and F. G. Garcia, "PAPR reduction via constellation extension in OFDM systems using generalized benders decomposition and branch-and-bound techniques," *IEEE Trans. Veh. Technol.*, vol. 65, no. 7, pp. 5133–5145, Jul. 2016.

[23] M. Laabidi and R. Zayani, "A quick convergence Active Constellation Extension Projection onto Convex Sets algorithm for reducing the PAPR of OFDM system", in International Conference on Advanced Information Networking & Applications Workshops, IEEE, 2016.

[24] Z. Zheng and G. Li, "An efficient FPGA design and performance testing of the ACE algorithm for PAPR reduction in DVB-T2 systems," *IEEE Trans. Broadcast.*, vol. 63, no. 1, pp. 134–143, Mar. 2017.

Yuzhuo Liu received the B.S. degree in Communication Engineering form Xidian University in 2014, and now he is studying for a M.S. degree in Xidian University. His research interests include wireless communication standards, such as 802.11ac WLAN, and PAPR reduction technique.

Yong Wang received the B.S., M.S. and Ph.D. degree from Xidian University, Xi'an, China in 1997, 2002 and 2005, respectively. He is now a professor of the State Key Laboratory of Integrated Services Networks, Xidian University, China. His research interests include wireless communication system and nonlinear signal processing.

Bo Ai (M'00-SM'09) received the M.S. and Ph.D. degree from Xidian University, Xi'an, China in 2002 and 2004, respectively. He graduated in 2007 with great honors of Excellent Postdoctoral Research Fellow in Tsinghua University. He is now working in Beijing Jiaotong University as a professor and advisor of Ph.D. candidates. He is a deputy director of State Key Laboratory of Rail Traffic Control and Safety. He is an associate editor for IEEE Trans. on Consumer Electronics and an editorial committee member of journal of Wireless Personal Communications. He has authored/co-authored 6 books, 26 invention patents and 130 scientific research papers in his research area till now. His current interests are the research and applications OFDM techniques, HPA linearization techniques, radio propagation and channel modeling, GSM Railway systems. He is an IEEE Senior member and a senior member of Electronics Institute of China (CIE).